RUC-MESSAGEix-China (RMC)

Model Documentation

School of Applied Economics, Renmin University of China

Oct, 2025 (Updating)

1. Overview

1.1. Background

The RUC-MESSAGEix-China (RMC) model is an energy-economy-environment (E3) integrated assessment model for China based on the open-source modeling framework MESSAGEix (IIASA ECE Programme, 2020). It has been co-developed and maintained by Prof. Zhou Wenji's group at the School of Applied Economics, Renmin University of China, and Prof. Ren Hongtao at the School of Business, East China University of Science and Technology.

1.2. Basic principles

The RMC model is based on the globally renowned integrated assessment modeling framework MESSAGEix, which is developed and maintained by the International Institute for Applied Systems Analysis (IIASA), and widely used for integrated assessment models (IAMs) and energy system models (ESMs) (IIASA ECE Programme, 2020). MESSAGEix is highly flexible and suitable for constructing local, national, multi-regional, or global energy system models, and can reflect the dynamic evolution of energy systems over multiple periods, as well as incorporate rich technological details. While typically used for analyzing energy systems at regional levels, this framework can also be applied to study individual energy sectors, such as electricity or heat.

As an optimization modeling framework, its mathematical principle involves an overall objective function to minimize the total discounted system cost over the whole modeling horizon, which aggregates the costs of all energy technologies, including investment and operating costs of technologies, extraction costs of exhaustible resources, and generation costs of renewable energy, emission taxes, and other expenditures. In addition, constraints can be added as needed, such as limiting total carbon emissions from the energy system (or carbon emissions from individual technologies).

More features and functions of MESSAGEix can be found in its online documentation¹ and related literature, e.g., (Huppmann *et al.*, 2019). The source code is available from the Git repository².

1.3. Spatial-temporal resolution

The RMC model currently covers 31 provincial-level administrative regions in mainland China (excluding Hong Kong, Macao, and Taiwan for now), accounting for the energy system structure, economic development patterns, and resource endowments, among other factors, at the provincial scale.

To assess the systemic impact of China's carbon-neutral goals, the current version of RMC is calibrated to 2022 and has a modeling horizon from 2025 to 2060 with a five-year time interval. Thanks to the flexibility of the MESSAGEix framework, both the time range and time step can be adjusted to meet various research needs.

3

¹ https://docs.messageix.org/en/latest/index.html

² https://github.com/iiasa/message_ix

2. The Reference Energy System

The reference energy system of the RMC model encompasses a comprehensive macro energy system supply chain, which can be divided into three stages: primary energy extraction, secondary energy processing and conversion, and final energy consumption (Figure 2-1). The energy demand sectors consist of three major end-use consumption categories: industry, buildings, and transportation. The industrial sector includes traditional energy-intensive industries such as iron and steel, cement, chemicals, general manufacturing, advanced manufacturing, and emerging sectors such as information technology. The transportation sector covers road transport, rail transport, shipping, aviation, etc., with detailed classifications of transport modes available in the relevant chapter of the RMC|Transport model. The building sector includes commercial facilities and residential households. Energy demand is represented in the model as useful energy and is exogenously determined based on socio-economic development projections. The above processes are illustrated in the modeling system structure shown in the figure below.

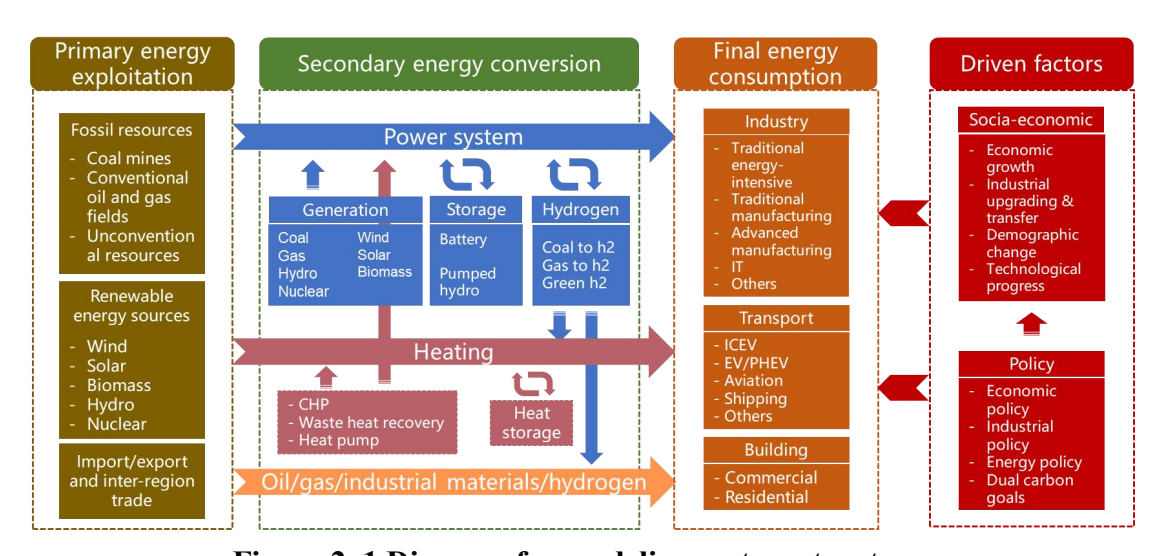


Figure 2-1 Diagram for modeling system structure.

There are two basic elements in the framework of MESSAGEix, namely energy technologies (also referred to as 'processes') and energy commodities. The interconversion and flow of energy commodities are linked through energy

technologies (processes), thereby constituting the different components of the energy system. Energy technologies are characterized by a detailed set of parameters. The figure below illustrates a simplified reference energy system within this framework, and shows the linkages between energy commodities and technologies. Note that this schematic does not include all technological routes (processes) or inter-regional energy flows covered by RMC.

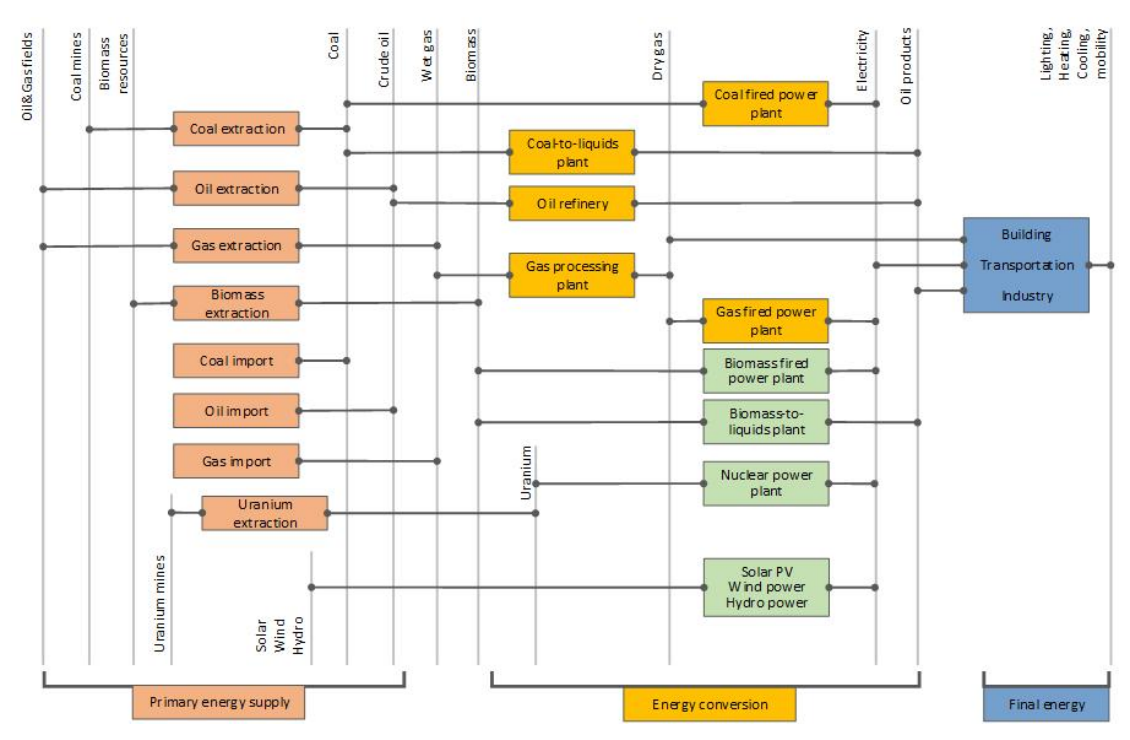


Figure 2-2 A simplified reference energy system.

The current version of the model involves over 400 energy technologies from energy supply to consumption, covering the full spectrum of energy supply: upstream resource extraction (resource supply), midstream processing and conversion (power plants, refineries, coking plants, etc.), energy transmission, import, and export.

2.1. Energy resource endowments

2.1.1. Fossil fuel reserves and resources

The accessibility and cost of fossil fuels play a critical role in shaping the future of the energy sector, thereby directly impact future climate mitigation pathways. It is imperative to understand the changes in the availability of fossil fuels and their extraction costs. The assumptions on fossil energy resources in RMC are derived from a large amount of sources, including national and global databases such as NBS and the United States Geological Survey (USGS), as well as reports and forecasts from diverse energy research institutes and organizations.

'Reserves' in this model refer to the quantities of fossil fuels proven through geological assessment with a significant degree of certainty regarding their existence (proven, probable, or possible) and can be commercially extracted under current economic and technological conditions. 'Resources', a broader concept than 'reserves', includes those that have not yet been discovered, as well as those that are technologically unfeasible or economically uncompetitive, but might be recoverable in the future, as well as those quantities that have geological potential for extraction, but yet to be found. Table 2-1 shows the calculated fossil fuel resources in the RMC model for 2022. Estimating fossil fuel reserves is built on technological assumptions. With an improvement in technology, the amount that may be considered a 'reserve' vs. a 'resource' can actually vary widely.

Table 2-1 Calculated results of China's fossil fuel resources in the RMC model.

Category	Resources (ZJ)
Coal	40
Conventional Oil	0.8
Unconventional Oil	0.6
Conventional Gas	1.6
Unconventional Gas	1.3

China's coal resources account for approximately 90% of total fossil resource estimates. Oil and natural gas are relatively scarce, with 1.4 ZJ and 2.9 ZJ resources, respectively.

Drawing from multiple sources of information, mainly from some literature and reports (McGlade and Ekins, 2015; China National Administration of Coal Geology,

2016; Li, 2019; Ministry of Natural Resources of the People's Republic of China, 2021; Welsby *et al.*, 2021), the supply costs of fossil fuels across the country have been estimated. Figure 2-3 presents the cumulative national resource supply curves for coal, oil, and gas in the RMC model. The blocks in different color shades indicate different resource categories.

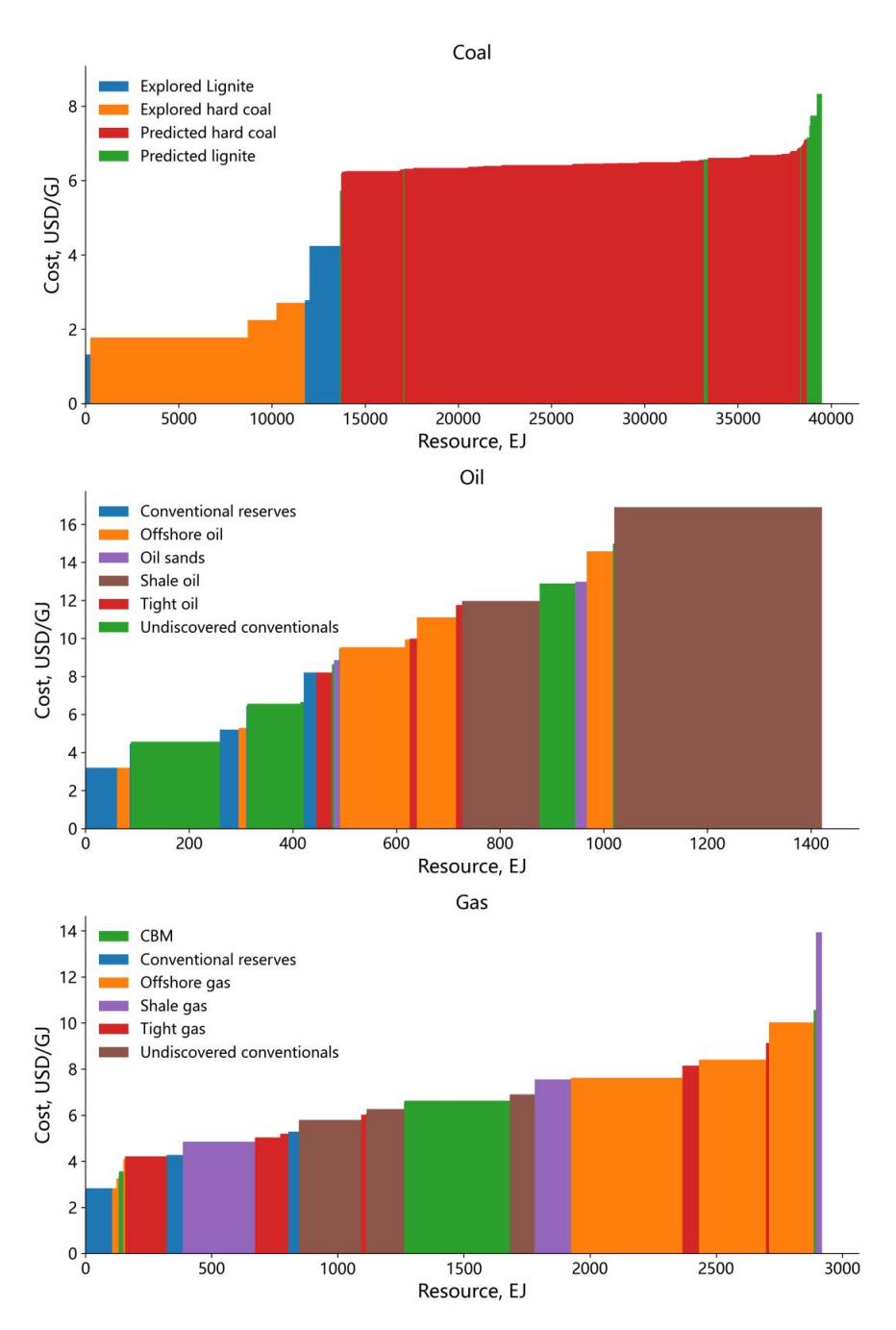


Figure 2-3 Cumulative national resource supply curves for coal (top), oil (middle), and gas (bottom) in the model.

Coal is the largest and most widely distributed fossil fuel resource in China. Every province except Shanghai has coal resources. In terms of spatial distribution, coal resources are more abundant in the north than in the south. Xinjiang and Inner Mongolia are the two regions with the largest coal resources, followed by Shanxi and Shaanxi. These four provinces in the north account for approximately 79% of the country's coal resources collectively. The distribution of conventional oil is also mainly in the northern regions, such as Xinjiang, Gansu, Shaanxi, Heilongjiang, and Shandong, all possessing more than 1 Gt of conventional onshore resources. Coastal provinces, including Hainan, Tianjin, and Guangdong, possess offshore oil resources. Unconventional oil, primarily in the form of shale oil, is highly concentrated and mainly distributed in Liaoning, Xinjiang, and Jilin. The distribution patterns of conventional and unconventional natural gas are similar, with Sichuan, Shaanxi, and Inner Mongolia rich in both resources. Thanks to its developed coal industry, Shanxi and Inner Mongolia also have a significant amount of coalbed methane (CBM) resources. Hainan and Guangdong have large offshore natural gas resources that are yet to be exploited. Figure 2-4 to Figure 2-11 show the regional distribution of different resource categories.



Figure 2-4 Regional distribution of remaining recoverable explored coal resources (Gt).



Figure 2-5 Regional distribution of remaining recoverable predicted coal resources (Gt).



Figure 2-6 Regional distribution of remaining recoverable conventional onshore oil (Gt).



Figure 2-7 Regional distribution of remaining recoverable offshore oil (Gt).



Figure 2-8 Regional distribution of remaining recoverable unconventional oil (Gt).



Figure 2-9 Regional distribution of remaining recoverable conventional onshore gas (Tcm).



Figure 2-10 Regional distribution of remaining recoverable offshore gas (Tcm).



Figure 2-11 Regional distribution of remaining recoverable unconventional gas (Tcm).

2.1.2. Biomass resources

Biomass energy is a potentially important renewable energy resource in the RMC model. This includes both commercial and non-commercial use. Commercial refers to the use of bioenergy in, for example, power plants or biofuel refineries, while non-commercial refers to the use of bioenergy for residential heating and cooking, primarily in rural households. The estimates of the national biomass resource potential in the model combine multiple sources (Zhang, 2018; Hanssen *et al.*, 2020; Kang *et al.*, 2020; Nie *et al.*, 2020; Biomass Energy Industry Promotion Association *et al.*, 2021; Tian *et al.*, 2021; Biomass Energy Industry Promotion Association and Energy Foundation, 2023; Wang Rui *et al.*, 2023). The biomass resources in the model include agricultural residues, forestry residues, energy crops, municipal sewage, municipal solid waste, and animal manure.

Table 2-2 shows the total volume, collectible volume, and energy utilization potential of China's biomass resources in the RMC model. The energy use potential is the amount obtained by deducting non-energy uses from the collectible volume. Relying on developed agriculture and animal husbandry, more than 60% of the national total biomass resources come from agricultural residues and animal manure. In southern provinces such as Guangxi and Yunnan, abundant forest resources also

provide considerable potential for biomass development. It is noteworthy that despite the substantial potential for growing energy crops across the country, the associated market and industry systems remain underdeveloped. Consequently, it is anticipated that a considerable period will be required for these crops to emerge as the primary source of biomass utilization within China.

Table 2-2 The scale and utilization potential of biomass resources in China (EJ).

Category	Total resource	Collectable resource	Energy use potential
Agricultural	15.3	13.3	4.2
Animal manure	22.7	22.7	7.6
Energy crops	16.0	16.0	16.0
Forestry	5.9	5.9	2.6
Municipal sewage	0.2	0.2	0.2
Municipal solid waste	1.7	1.7	1.7

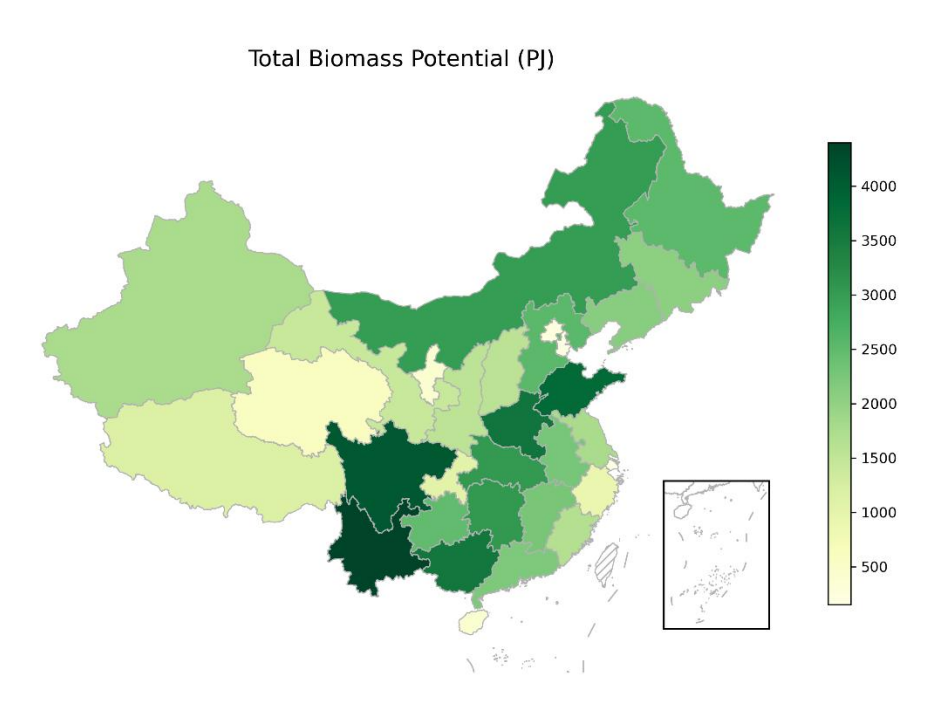


Figure 2-12 Regional distribution of total biomass potential (PJ).

2.1.3. Wind and Solar Resources

Wind and solar energy, as clean and renewable sources, are of strategic importance for China to achieve its carbon neutrality goal by 2060. Currently, China's installed capacity of wind and solar power ranks among the highest in the world, yet the development level remains relatively low, accounting for only a small fraction of its vast technical potential, indicating substantial room for growth in resource utilization. The model calibrates the potential of wind and solar resources across provinces by referencing multiple sources, including GIS-based refined assessment studies and annual reports from the China Meteorological Administration (Wang *et al.*, 2022; Chinese Academy of Environmental Planning, 2024; China Meteorological Administration, 2025).

Spatially, wind-rich areas are primarily concentrated in western, northern, and coastal provinces, while solar resources are predominantly located in the western and northern regions, with the 'three north' area hosting the majority of the national potential. Specifically, the national technical potential for wind power is approximately 10.9 TW, and for solar power, about 45.6 TW. Overall, China possesses abundant renewable energy resources sufficient to support its energy transition, and future macro-level planning for wind and solar energy bases, along with distributed development, should focus on key regions.

Table 2-3 Wind and solar power resource potential by province.

Installed Capacity (GW)						Generation (TWh)		
Region	Wind	Onshore wind	Offshore wind	PV	Central PV	Distributed PV	Wind	PV
Inner Mongolia	2697	2697	0	9460	9230	230	7143	14167
Heilongjiang	706	706	0	301	149	152	1937	394
Jilin	304	304	0	356	243	113	861	466
Liaoning	289	176	113	191	17	174	777	238
Gansu	321	321	0	2758	2682	76	718	4128
Ningxia	82	82	0	282	253	29	241	391

Qinghai	186	186	0	3914	3886	28	379	6491
Shanxi	165	165	0	372	298	75	448	458
Xinjiang	618	618	0	21198	21054	144	1293	29265
Beijing	0	0	0	61	2	59	0	72
Hebei	334	281	53	338	59	279	988	587
Shandong	596	296	300	417	21	395	1636	552
Shanxi	127	127	0	311	194	117	364	439
Tianjin	15	11	4	42	0	42	42	50
Chongqing	43	43	0	22	1	21	108	3
Guizhou	109	109	0	104	76	28	296	105
Sichuan	223	223	0	157	75	82	621	182
Xizang	524	524	0	3332	3327	4	1375	6177
Guangdong	677	141	536	202	19	182	1977	257
Guangxi	250	181	69	187	101	86	708	222
Hainan	246	45	201	29	10	19	563	33
Yunnan	132	132	0	115	60	55	374	159
Henan	291	291	0	303	14	289	869	377
Hubei	206	206	0	157	33	124	558	188
Hunan	174	174	0	91	9	83	462	96
Jiangxi	152	152	0	97	27	70	423	109
Anhui	225	225	0	233	11	222	679	280
Fujian	321	32	289	91	18	73	957	102
Jiangsu	441	177	264	302	5	297	1200	372
Shanghai	55	10	45	38	0	37	150	51
Zhejiang	429	50	379	112	4	108	1163	121
National	10948	8694	2254	45604	41878	3726	29308	66529

2.2. Power System

The RMC model covers a full range of electricity generation, transmission, and storage in and between the 31 provinces' power systems. It can run with an annual

time resolution consistent with other modules and or be linked with a dedicated power system model CPOST with an hourly resolution (8760 hours for a modeled year) to capture more detailed characteristics in the power system. The spatial resolution and technologies in the power system are consistent between RMC and CPOST. Description of the CPOST model is available from its documentation (Renmin University of China, 2025).

2.2.1. Generation technologies

The power system encompasses a variety of power generation technologies, including fossil fuel-based generation, nuclear, and renewable energy like hydro, wind, solar, and biomass power generation, along with energy storage and transmission infrastructures.

In coal-fired power generation, there are advanced technologies such as large ultra-supercritical and supercritical units, as well as relatively low efficient subcritical technologies. Gas-fired power generation includes large combined cycle gas turbine (CCGT) units and conventional open-cycle gas turbine (OCGT). The system has also taken into account the integration of carbon capture and storage (CCS) technology within power generation units. The following shows the list of generation technologies, including both fossil and renewables in the model.

- Coal w/o CCS: ultra-supercritical units (USC), supercritical units (SC), and subcritical units (Sub-C);
- Coal w/ CCS: ultra-supercritical units with CCS, supercritical units with CCS;
- Gas w/o CCS: combined cycle gas turbine (CCGT) and open cycle gas turbine (OCGT);
- Gas w/ CCS: CCGT with CCS and OCGT with CCS;
- Biomass w/ CCS;
- Biomass w/o CCS;
- Solar: centralized/distributed photovoltaic (PV) power station and solar thermal power plant (concentrated solar power, CSP);

- Wind: onshore/offshore wind;
- Nuclear.

Note that CCS is treated as an 'add-on' technology to the parent technology, e.g., coal-fired ultra-supercritical units or biomass power plants. More details on how CCS is modeled can be found in the MESSAGEix document.

2.2.2. Capital costs

Table 2-4 shows the cost trajectory of power generation technologies in a baseline scenario with references to several studies (McElroy *et al.*, 2009; Lu *et al.*, 2021; IEA, 2022, 2023b, 2023a, 2024; National Bureau of Statistics of China, 2022, 2023, 2024; Wang *et al.*, 2022; China Meteorological Administration, 2023; Ember, 2023; CEIC, 2024; Dianchacha, 2024; EMBER, 2024). The model allows for adjustments to the cost of each specific generation technology in different scenario designs.

Table 2-4 Capital cost assumptions for generation technologies in RMC (unit: US\$/kW).

Technology	2025	2030	2035	2040	2045	2050	2055	2060
Coal w/o CCS	631	606	583	563	546	533	523	514
Coal w/ CCS	1015	932	860	798	753	719	695	668
Gas w/o CCS	325	315	306	298	291	286	282	278
Gas w/ CCS	678	617	564	519	487	463	446	427
Hydro	2168	2059	1966	1873	1873	1873	1873	1873
Nuclear	2311	2242	2173	2103	2034	1965	1910	1865
Solar PV (distributed)	393	336	279	256	235	216	201	189
Solar PV (central)	493	394	296	272	251	232	217	205
Solar PV (thermal)	2329	1491	1400	1309	1227	1154	1095	1048
Onshore wind	600	521	489	457	428	402	378	360
Offshore wind	1383	1047	808	778	750	726	706	690
Biomass w/o CCS	1290	1231	1191	1150	1113	1080	1053	1032
Biomass w/ CCS	2321	2108	1936	1784	1668	1580	1515	1445
Battery storage	824	798	773	764	757	750	744	740

Pumped-hydro storage	1237	1090	1002	949	917	898	889	884
UHV transmission	329	325	315	306	299	296	295	295

2.3. Other energy conversion

Similar to the power system, several district heating technologies based on fossil and renewable energy sources are considered in the RMC model. These heating plants feed heat into the district heating system that is then used in the end-use sectors.

Beyond electricity and centralized heat generation, there are three further subsectors of the conversion sector represented in the model, namely, liquid fuel production, gaseous fuel production, and hydrogen production.

In addition to oil refining, the main supply technology for liquid fuels currently, the model also encompasses a variety of alternative pathways for producing liquid fuels from diverse feedstocks, such as coal liquefaction, gas-to-liquids technologies, and biomass-to-liquids technologies, with and without the integration of CCS. Gaseous fuel production technologies cover biomass gasification and coal gasification. Hydrogen production includes gasification processes for coal and biomass, steam methane reforming from natural gas, and water electrolysis.

2.4. Technological advancement

In the RMC model, technological advancements are considered as exogenous factors and vary across scenarios. However, related studies have been conducted to incorporate the endogenous aspects of technological change through learning curves within energy-engineering models, as well as to examine how technology costs are influenced by market structures.

Cost and performance parameters, such as conversion efficiencies and emission factors, are typically sourced from the extant engineering studies. At the same time, alternative projections for costs and performance are formulated to account for a broad spectrum of uncertainties that significantly impact the model results for the future.

2.5. Energy demand

Energy service demands from end-use sectors such as industry, transportation, and residential/commercial are calculated with socio-economic development projections and exogenous to RMC. These demands are generated through the utilization of a scenario generator implemented in Python. The scenario generator correlates historical GDP per capita to final energy demands at the regional level. It extrapolates the sectoral energy service demands into the future, by leveraging projections of GDP and population growth. The scenario generator runs regressions on the historical datasets to establish the relationship for each of the 31 RMC regions between the independent variable (GDP per capita) and factors such as total final energy intensity, shares of final energy among several energy end-use sectors, and shares of electricity use between the industrial and residential/commercial sectors. With the input parameters, both the final energy intensity and the sectoral distribution can be projected.

Sector-specific models are under development and expected to link with the main RMC model in different ways.

3. Socio-economic drivers

Population and economic development levels exert profound influences on the capacity to mitigate and adapt to climate change (O'Neill *et al.*, 2014). Demographic change and economic growth are the key determinants of future energy demand in the RMC model, and are exogenous to the model.

3.1. Population

The demographic change for each region is calculated with reference to the projection from Chen et al and the United Nations World Population Prospects(Chen et al., 2020; UN DESA/Population Division, 2024). Chen et al estimated China's provincial population from 2010 to 2100 by age (0 to above 100), sex (male/female), and educational levels (illiterate, primary school, junior-high school, senior-high school, college, bachelor's, and master's and above) under five shared socioeconomic pathways (SSP1-5). Our study uses the SSP2 projection as the benchmark, which represents an intermediate path where future development follows the historical pattern(O'Neill et al., 2017). As the projection from Chen et al. starts in 2010 and does not include the latest trend, the data from the National Bureau of Statistics (NBS) and the demographic projection for the whole country from UN World Population Prospects are used to calibrate and update the province-level projections. The results show that China's national population peaks at 1.4 billion people in 2021, and slowly declines thereafter, falling to 631 million by the end of the century. Figure 3-1 shows the calibrated population change for each region in the model. Aligning with the original results from (Chen et al., 2020), the calibrated demographic results differentiate between rural and urban demographics and additionally take into account varying household income levels and energy consumption structures.

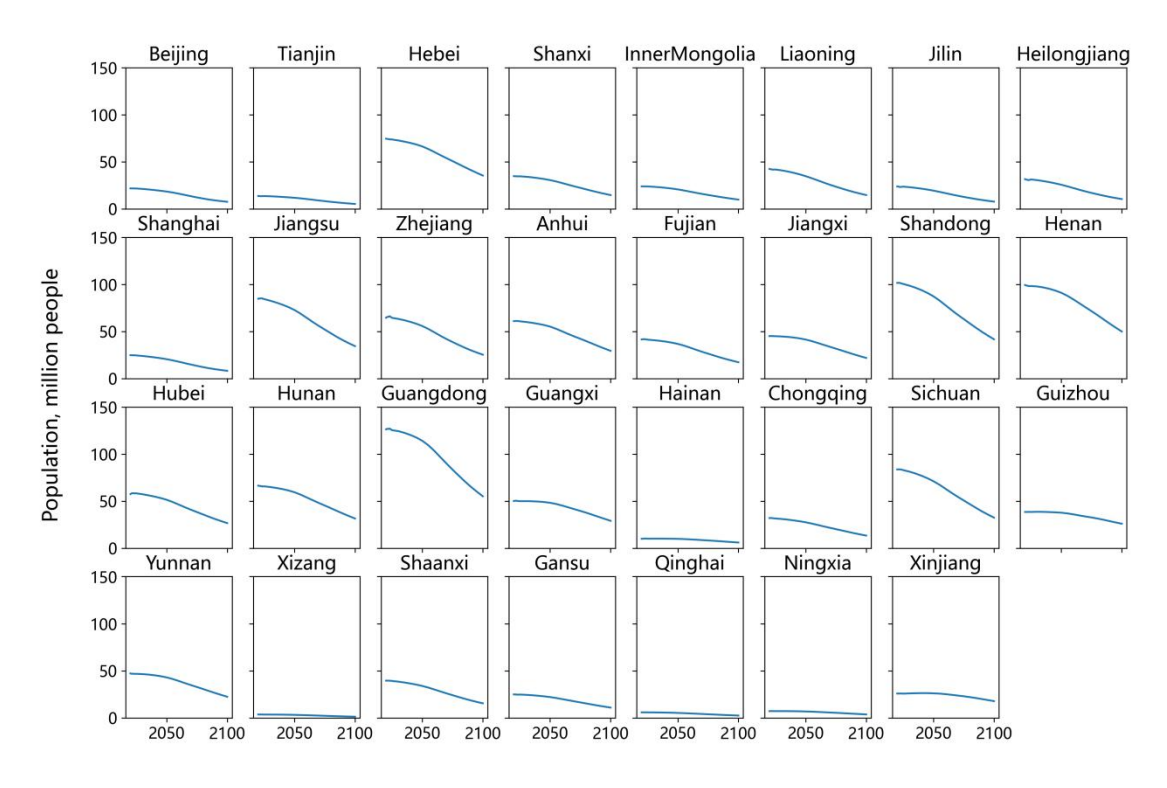


Figure 3-1 Provincial trends of total population in China from 2020 to 2100.

3.2. Economic growth

The future economic growth at the provincial level used in the model is obtained from the GDP projections from relevant literature (Bai and Zhang, 2017; Leimbach *et al.*, 2017; Christensen, Gillingham and Nordhaus, 2018; Pan *et al.*, 2020; Jing *et al.*, 2022; Yang *et al.*, 2024). The changes in GDP per capita in each region can be further derived from the projections of population and GDP. The average income is projected to grow by a factor and exceed 100 thousand USD/capita by the end of the century. Figure 3-2 and Figure 3-3 depict a future of progress where the provinces achieve significant economic growth, with incomplete economic convergence across different regions.

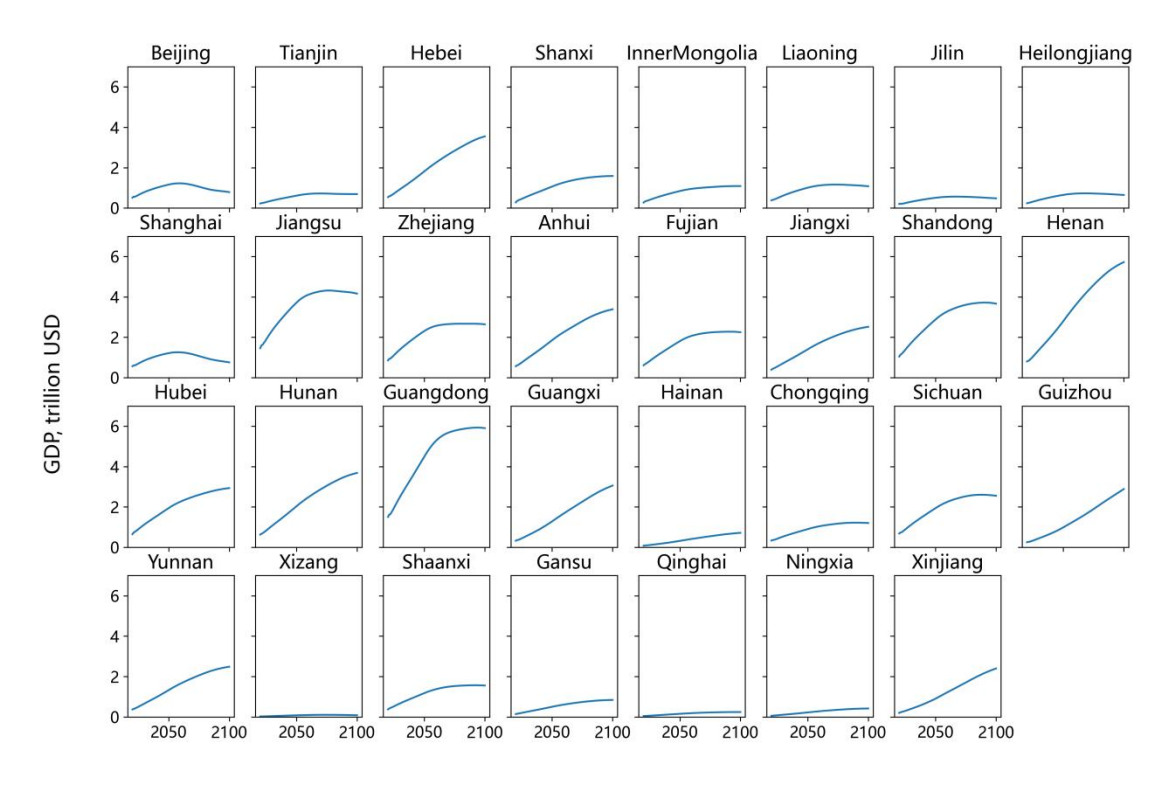


Figure 3-2 Provincial trends of GDP in China from 2020 to 2100.

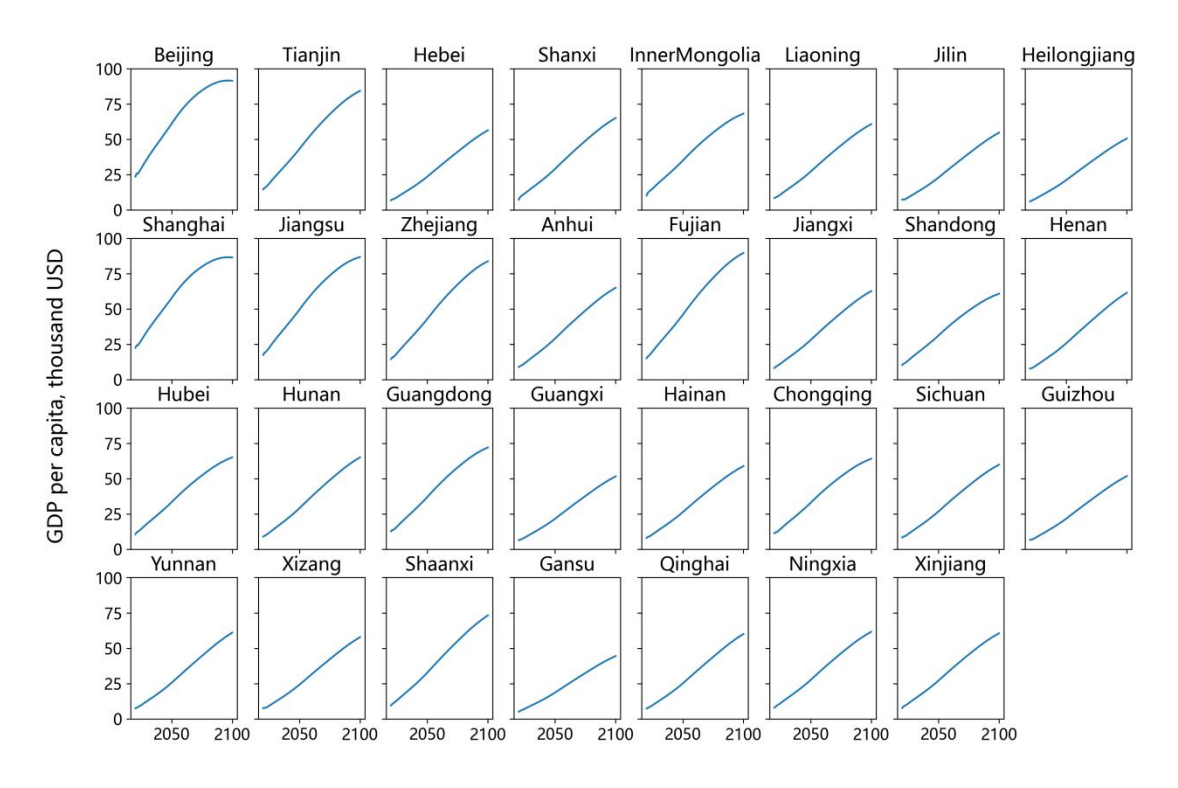


Figure 3-3 Provincial trends of GDP per capita in China from 2020 to 2100.

4. Iron and steel module: RMC|Steel

The RUC-MESSAGEix-China|Steel (RMC|Steel) model is the steel-industry module within the RMC model family. It is designed to analyze the evolution of supply and demand, technological composition, energy structure, and the demand for specific energy carriers (such as hydrogen) in China's steel industry during its low-carbon transition. The model covers 31 provincial-level administrative regions in mainland China. It incorporates, in a bottom-up manner, the major production processes and key technological details of the steel sector, and has been calibrated using empirical historical data on production capacity, output, and technology costs.

4.1. Model structure

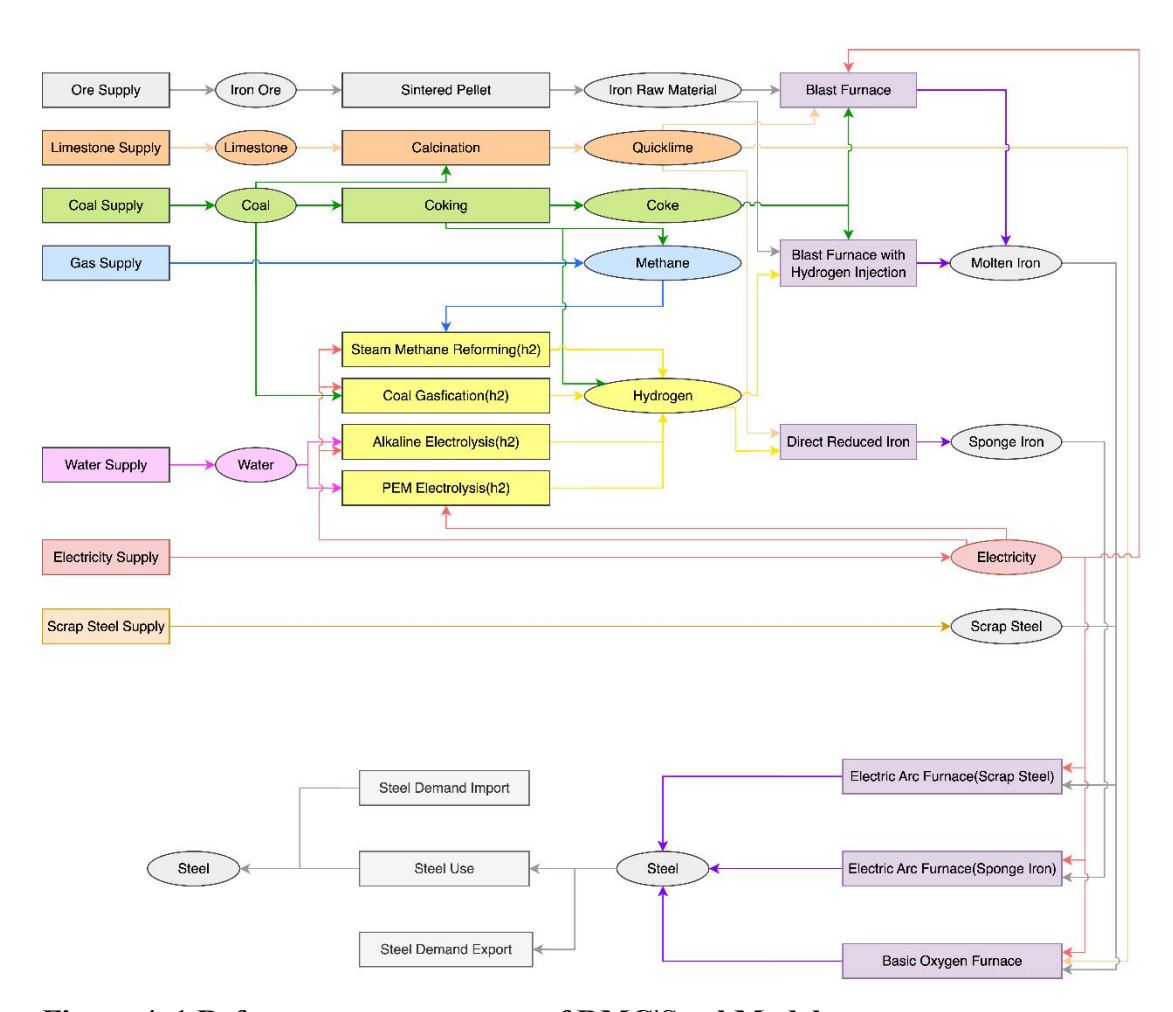


Figure 4-1 Reference energy system of RMC|Steel Model.

As shown in Figure 4-1, the RMC|Steel model mainly models raw material processing, pig iron smelting, and crude steel smelting, and does not involve the subsequent processing of steel coils, billets, and other products. Among them, raw material processing mainly includes:

- (1) Coking (coking)
- (2) Calcination of limestone (calcin)
- (3) Sintering and pelletizing of iron ore (sint pelle)

The principal ironmaking technologies include:

- (1) Blast furnace ironmaking (bf)
- (2) Hydrogen-enriched blast furnace ironmaking (bf h2)
- (3) Natural gas-based direct reduced iron (dri)
- (4) Hydrogen-based direct reduced iron (hdri)
- (5) Hydrogen-based direct smelting reduction (hmr)

The main steelmaking technologies include:

- (1) Basic oxygen furnace steelmaking (bof)
- (2) Electric arc furnace steelmaking using scrap as the primary feedstock (eaf_scrap)
 - (3) Electric arc furnace steelmaking using DRI as the main feedstock (eaf spg)

For BF, DRI, and BOF facilities, carbon capture and storage (CCS) technologies can be incorporated to mitigate CO₂ emissions. The BF facilities can also be retrofitted with hydrogen injection systems to achieve partial hydrogen substitution. In addition, the model provides a detailed breakdown of hydrogen production pathways, distinguishing among coal gasification, natural gas reforming, and water electrolysis from a technological perspective, each of which can be coupled with corresponding CCS technologies.

The input–output relationships among these major processes and technologies are summarized in Table 4-1.

Table 4-1 RMC|Steel main technology input and output.

Technology	Imput	Output
Blast furnace	coke, elec, i_raw, qklime	i_molt
Direct reduced iron	h2, i_raw	i_spg
Basic oxygen furnace	i_molt, elec, qklime	steel
Electric arc furnace (sponge iron)	i_spg, elec	steel
Electric arc furnace (scrap)	scrap	elec
Coal-based hydrogen production	coal, elec	h2
Natural gas-based hydrogen production	ch4, elec	h2
Electrolysis-based hydrogen production	elec, water	h2

4.2. Parameter settings

4.2.1. Capital expenditures (CAPEX)

Technology	CAPEX	Unit	Data source
Sintering/pelletizing	45.87	M\$/Mtpa ³	Steelonthenet, 2023
Limestone Calcination	109.6	M\$/Mtpa	Chumin, 2025
Coking	446.2	M\$/Mtpa	Reliable Plant, 2008
BF iron-making	211	M\$/Mtpa	IEA-ETSAP, 2010a
BF w/ H ₂ injection	40	M\$/Mtpa	-
BF w/ CCS	80.24	M\$/Mtpa	He et al., 2025; Wang et al., 2025
H-DRI	580	M\$/Mtpa	Christoph Heinemann et al., 2024
BOF steel-making	100	M\$/Mtpa	IEA-ETSAP, 2010
BOF w/ CCS	80.24	M\$/Mtpa	He et al., 2025
EAF (using DRI as main feedstock)	143	M\$/Mtpa	Steelonthenet.com, 2025
EAF (using scrap as main feedstock)	143	M\$/Mtpa	Steelonthenet.com, 2025
Coal to H ₂	10692	M\$/Mtpa	IEA, 2020; Energy Transitions Commission, 2023
Coal to H ₂ w/ CCS	444	M\$/Mtpa	IEA, 2020
Gas to H ₂	3641.3	M\$/Mtpa	IEA, 2020
Gas to H ₂ w/ CCS	2693 (1488.5 in 2050)	M\$/Mtpa	IEA, 2020
Electrolysis	8296.5 (3583.1 in 2050)	M\$/Mtpa	IEA, 2020

³ tpa: tons per annum.

4.2.2. Fixed operation expenditures

Technology	Fixed OPEX	Unit	Data source
Sintering/pelletizing	1.835	M\$/Mtpa	Arasto, 2015
Limestone Calcination	8.05	M\$/Mtpa	AGICO Cement Plant Equipment, 2025
Coking	17.18	M\$/Mtpa	Gallaher, Depro and Agency, 2002
BF iron-making	14.14	M\$/Mtpa	Gallaher, Depro and Agency, 2002; IEA, 2013
BF w/ H ₂ injection	10	M\$/Mtpa	-
BF w/ CCS	4.07	M\$/Mtpa	IEA, 2013
H-DRI	20	M\$/Mtpa	Steelonthenet.com, 2025
BOF steel-making	15.45	M\$/Mtpa	IEA Greenhouse Gas R&D Programme, 2024
BOF w/ CCS	2.16	M\$/Mtpa	IEA, 2013
EAF (using DRI as main feedstock)	81.24	M\$/Mtpa	Vogl, Åhman and Nilsson, 2018; Benavides <i>et al.</i> , 2024
EAF (using scrap as main feedstock)	81.24	M\$/Mtpa	Vogl, Åhman and Nilsson, 2018; Benavides <i>et al.</i> , 2024
Coal to H ₂	433	M\$/Mtpa	Shao Le <i>et al.</i> , 2024
Coal to H ₂ w/ CCS	18	M\$/Mtpa	/
Gas to H ₂	454.5	M\$/Mtpa	Shao Le <i>et al.</i> , 2024
Gas to H ₂ w/ CCS	50.2	M\$/Mtpa	/
Electrolysis	182.5	M\$/Mtpa	IEA, 2020

4.2.3. Variable operation expenditures

Technology	Variable OPEX	Unit	Data source
Iron ore supply	110.61	M\$/Mt	Trading Economics, 2025
Limestone supply	19.59	M\$/Mt	kq81.com, 2025
Coal supply	195.89	M\$/Mt	National Bureau of Statistics of China, 2025
Natural gas supply	694	M\$/Mt	CEIC Data, 2025
Electricity supply	0.085	M\$/GWh	State-owned Assets Supervision and Administration Commission of the State Council, 2020
Water supply	0.676	M\$/Mt	CEIC Data, 2025
Scrap supply	349.8	M\$/Mt	CSteelNews, 2025
Sintering/pelletizing	20	M\$/Mt	Rahbari et al., 2025
Coal to H ₂	434.1	M\$/Mt	Shao Le <i>et al.</i> , 2024
Coal to H ₂ w/ CCS	0	M\$/Mt	/
Gas to H ₂	338.5	M\$/Mt	Shao Le <i>et al.</i> , 2024
Gas to H ₂ w/ CCS	0	M\$/Mt	/
Electrolysis	0	M\$/Mt	/

4.2.4. Carbon emission factors

Technology	Emission factor	Unit	Data source
Sintering/pelletizing	0.2	t-CO ₂ /t-output	CSteelNews, 2023; Steelonthenet, 2025; ZHAO Zedong, LI Jiaxuan, and LI Yuanye, 2025
Limestone Calcination	1	t-CO ₂ /t-output	Shenlan Environmental Protection Industry Development Co., Ltd., 2025
Coking	0.794	t-CO ₂ /t-output	Steelonthenet, 2025
BF iron-making	1.22	t-CO ₂ /t-output	Steelonthenet, 2025
BF w/ H ₂ injection	0.67	t-CO ₂ /t-output	Zhang et al., 2024; OECD, 2025
BF w/ CCS	0.0523	t-CO ₂ /t-output	Santos et al., 2013
H-DRI	0.04	t-CO ₂ /t-output	Rechberger et al., 2020
BOF steel-making	0.181	t-CO ₂ /t-output	Nancy Margolis and Ross Brindle, 2000; European Commission. Joint Research Centre., 2022; steelonthenet, no date
BOF w/ CCS	0.03	t-CO ₂ /t-output	Butterworth, 2024
EAF (using DRI as main feedstock)	0.03	t-CO ₂ /t-output	European Commission. Joint Research Centre., 2022
EAF (using scrap as main feedstock)	0.03	t-CO ₂ /t-output	European Commission. Joint Research Centre., 2022
Coal to H ₂	20.1	t-CO ₂ /t-output	IEA, 2019
Coal to H ₂ w/ CCS	2.1	t-CO ₂ /t-output	IEA, 2019
Gas to H ₂	10.13	t-CO ₂ /t-output	Baltac et al., 2022
Gas to H ₂ w/ CCS	2.32	t-CO ₂ /t-output	Baltac et al., 2022

5. Transport module: RMC|Transport

RMC|Transport is a module within the RMC model family focused on the transportation sector, designed to analyze supply-demand dynamics, technology and energy mix, carbon emissions, and other impacts (such as critical metal demand) during the low-carbon transition of China's transportation sector. Different from the main RMC model, the transportation module employs a stock-flow system dynamics approach. Its geographical coverage includes 31 provincial-level administrative units in mainland China. It incorporates, in a bottom-up manner, major production processes and key technological information relevant to the transportation sector, and has been calibrated based on historical data for vehicle stocks, activity levels, and technology costs.

5.1. Model structure

As shown in Figure 5-1, RMC|Transport primarily covers the road transport sector (with future extensions planned for shipping, rail, and other transport sectors). This includes private vehicles, commercial vehicles, public service vehicles, and other road transport. The energy types considered in the model include gasoline, diesel, electricity, hydrogen, natural gas, and other alternative fuels.

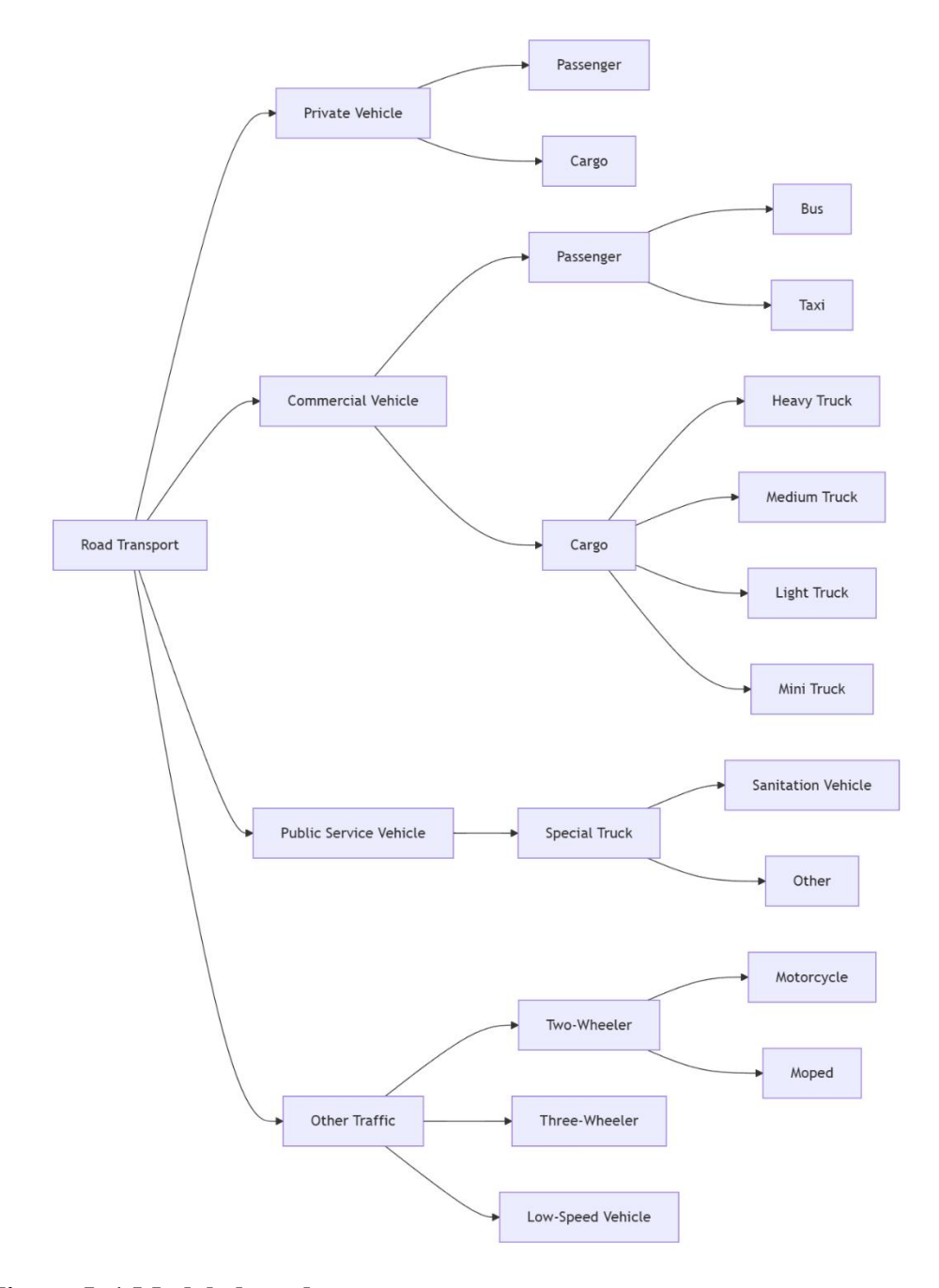


Figure 5-1 Modeled road transport sector.

5.2. Modelling vehicle stocks and flows

The model utilizes a system dynamics approach to analyze the stock-flow relationships of private passenger cars. Let $V_{f,c,a}(t)$ denote the stock of private passenger cars in year t, with fuel type f, vehicle type c, and vehicle age a. Aggregating over age groups gives $V_{f,c}(t) = \sum_{a=0}^{A} V_{f,c,a}(t)$. The total stock N(t) is

defined as the sum of stocks across all fuel-body type combinations, i.e., $N(t) = \sum_{f,c} V_{f,c}(t)$.

Denoting the new registrations of private passenger cars in year t as $n_{f,c}(t)$, and the number of vehicles retired due to reaching end-of-life as $r_{f,c,a}(t)$, the stock-flow relationship is expressed as:

$$\Delta V_{f,c}(t) = n_{f,c}(t) - \sum_{a=0}^{A} r_{f,c,a}(t)$$
 (5-1)

where the retirements satisfy:

$$r_{f,c,a}(t) = \alpha_{f,c,a}(t) \cdot V_{f,c,a}(t) \tag{5-2}$$

Here, $\alpha_{f,c,a}(t) \in [0,1)$ is the retirement risk coefficient for the specific vehicle type.

The national per capita private passenger car stock $\overline{N}(t)$ follows a GDP-enhanced Gompertz curve:

$$\overline{N}(t) = \gamma_{max} \cdot \exp\left(-K \cdot \exp\left(-B \cdot G(t)\right)\right) + \theta \cdot \overline{N}(t-1)$$
 (5-3)

where γ_{max} is the saturation level, G(t) is the per capita GDP, positive constants K and B are the shape and location parameters of the curve, respectively, and the coefficient $\theta \in [0,1]$ adjusts for the inertia effect of the per capita stock and the income effect. Based on this, the absolute stock level N(t) is obtained using the population POP_t :

$$N(t) = \overline{N}(t) \cdot POP_t \tag{5-4}$$

To ensure consistency between macro and micro levels, the annual net change in the private passenger car stock $\Delta N_t = N(t+1) - N(t)$, the total new registrations $n_t = \sum_{f,c} n_{f,c}(t)$, and the total retirements $R_t = \sum_{f,c,a} r_{f,c,a}(t)$ must satisfy:

$$\Delta N_t = n_t - R_t \tag{5-5}$$

At the fleet level, the recursive relationship with a one-year time step is as follows:

$$V_{f,c,a+1}(t+1) = (1 - \alpha_{f,c,a}(t)) \cdot V_{f,c,a}(t) \ \forall a \ge 0$$
 (5-6)

$$V_{f,c,0}(t+1) = n_{f,c}(t) (5-7)$$

Vehicle lifetime is assumed to follow a Weibull distribution to reflect the empirical pattern that older vehicles are retired more frequently. The retirement risk coefficient can then be calculated from the Weibull distribution parameters:

$$\alpha_{f,c,a} = 1 - \frac{S(a+1)}{S(a)} = 1 - \exp\left(-\left[\left(\frac{a+1}{h_{f,c}}\right)^{s_{f,c}} - \left(\frac{a}{h_{f,c}}\right)^{s_{f,c}}\right]\right)$$
 (5 - 8)

Alternatively, log-normal or Gamma distributions can be used for simplification.

The projection results for the ownership of private passenger cars are shown in Figure 5-2. Currently, the number of private passenger cars per 100 people shows a significant positive correlation with economic development levels. Economically developed regions like Zhejiang, Jiangsu, and Beijing all exceed 24 vehicles per 100 people, while provinces such as Jiangxi, Hunan, and Gansu have approximately 15 vehicles per 100 people. In the future, the growth of the car stock in first-tier cities is projected to be slower, approaching or reaching saturation levels after 2050, while other regions will maintain relatively faster growth rates.

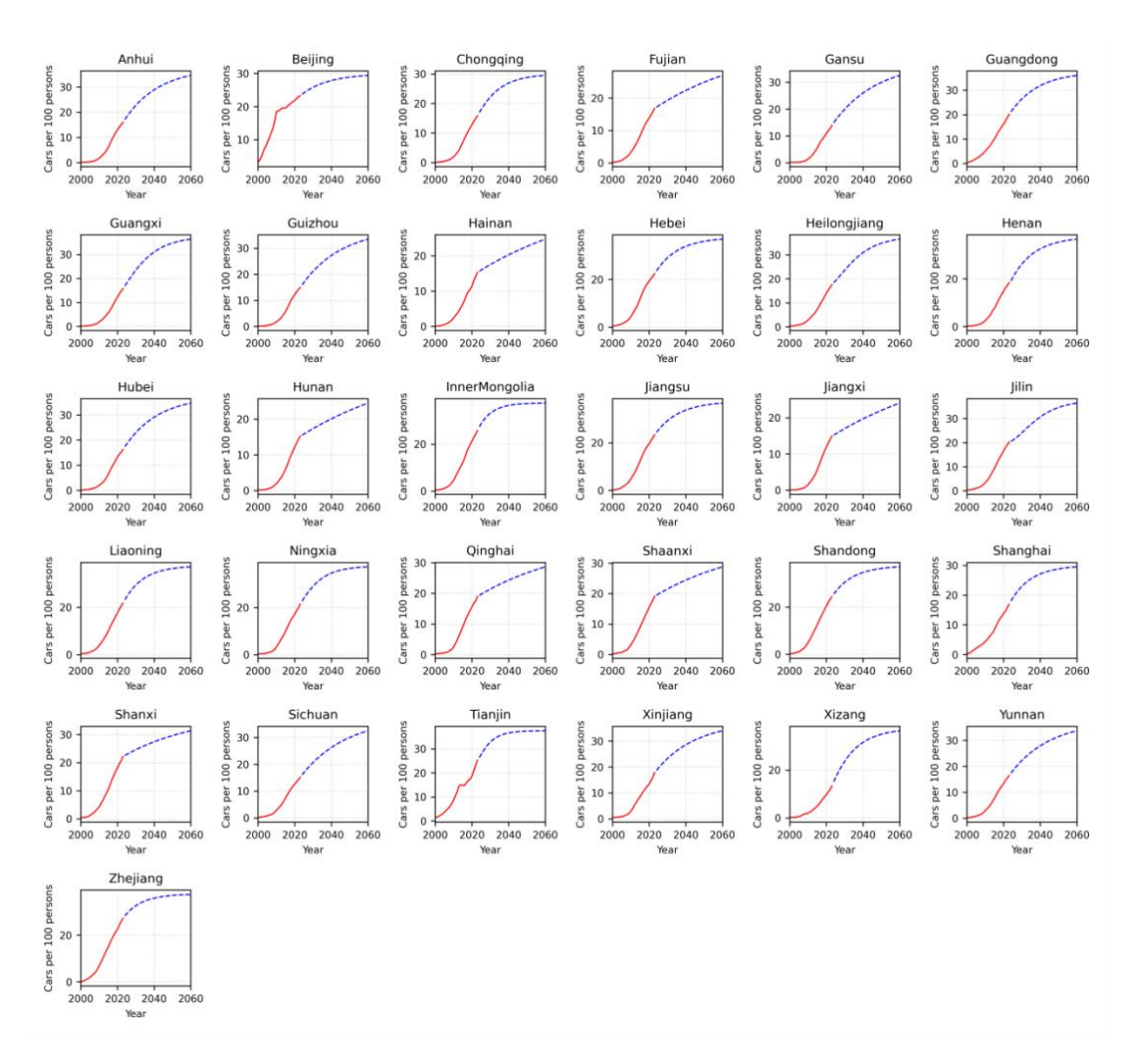


Figure 5-2 Ownership of private passenger cars per 100 inhabitants by province (2000-2060).

5.3. Consumer choice for private passenger vehicles

The selection of private passenger cars is driven by multiple factors, primarily including the vehicle purchase price, per-100-kilometer energy cost, driving range, and refueling/recharging convenience. These factors collectively shape consumer decision-making behavior, and their interrelationships are illustrated in Figure 5-3.

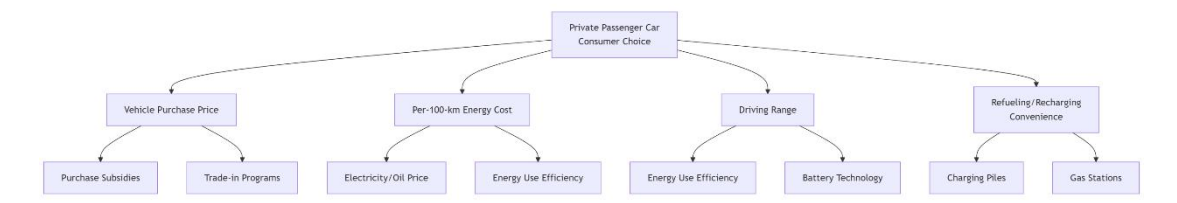


Figure 5-3 Main factors influencing the choice of private passenger vehicles.

5.3.1. Vehicle purchase price

The vehicle purchase price refers to the total cost actually paid by the consumer, encompassing the Manufacturer's Suggested Retail Price (MSRP), the influence of policy incentives, and market conditions. The final price paid by the consumer equals the sum of the MSRP, insurance, and license plate costs, minus dealer discounts, local subsidies, and consumption vouchers.

The evolution of this parameter is primarily driven by local government subsidy policies (e.g., national and local subsidies) and license plate costs in cities with purchase restrictions. Provincial-level discount coefficients for BEVs and PHEVs are set based on historical data (implementation of subsidy policies from 2017 to 2021). For instance, the local subsidy was approximately one thirds the national subsidy in 2019 and 10% in 2020, respectively, and phased out to zero in 2021. Future price pathways are described using the price change rate parameter $\delta_{i,f}$:

$$P_f(t) = P_f(t_0) \cdot \prod_{i=t_0}^t (1 + \delta_{i,f})$$
 (5 – 9)

where $P_f(t)$ is the purchase price of a vehicle of fuel type f in period t, and $P_f(t_0)$ is the purchase price of that vehicle type in the base year.

Table 5-1 Phased change trend of purchase price.

Fuel type	2025–2030	2030–2045	2045–2060
BEV	Rapid decline (battery cost-driven)	Stabilization or slow decline (marginal improvements)	Most affordable
PHEV	Slight decline (dependent on dual systems)	Remains basically stable	Demand decreases → Price rebounds or product exits market
GASL	Remains stable or increases slightly	Accelerated increase (rising environmental costs)	Sharp decrease → Price structure becomes
DIESEL	Slight increase (due to restrictions)	Significant increase (ban on sales/use)	Basically exits the market

Table 5-2 Price change rate of different fuel types.

Fuel type	2025–2030	2030–2045	2045–2060
BEV	_5%/yr	-1.5%/yr	-0.5~0%/yr
PHEV	-2%/yr	0%/yr	1%/yr
GASL	0~1%/yr	2%/yr	3~4%/yr
DIESEL	1%/yr	4%/yr	5%/yr

5.3.2. Fuel efficiency

Vehicle fuel efficiency is measured by the monetary value of energy consumed per 100 km driven. For BEVs, it is the product of electricity consumption per 100 km and the electricity price; for gasoline/diesel vehicles (GASL/DIESEL), it is the product of fuel consumption per 100 km and the fuel price; for PHEVs, a comprehensive calculation is required. The formula is as follows:

$$C_{p,k}(t) = EC_{p,k}(t) \cdot \alpha_{p,k} \cdot P_{p,k}^{\text{fuel}}(t)$$
 (5 – 10)

Here, $C_{p,k}(t)$ is the cost for province p and vehicle type k in period t, $EC_{p,k}(t)$ is the NEDC standard energy consumption, $\alpha_{p,k}$ is a province-specific adjustment coefficient, and $P_{p,k}^{\text{fuel}}(t)$ is the fuel price per unit. BEV energy efficiency is modeled based on an S-curve technological diffusion path derived from IEA physical limits. Fuel consumption for internal combustion engine vehicles remains stable. PHEV fuel consumption is constant, with efficiency improvements relying on increased electric range. Fuel price evolution is based on a green transition scenario: electricity prices first rise, then fall due to renewables, while oil prices experience a long-term moderate increase due to carbon taxes.

5.3.3. Driving range

Driving range refers to the maximum distance a vehicle can travel on a full energy supply and is a key consideration for NEV users. The range for conventional vehicles is assumed constant. The range for NEVs is determined by cell energy density $ED_{f=NEV}(t)$, battery pack mass M_{pack} , battery pack integration efficiency $\eta_{\text{pack}}(t)$, and energy consumption $EC_{p,f=NEV}(t) \cdot \alpha_{p,f=NEV}$:

$$Range_{p,f=\text{NEV}}(t) = \frac{ED_{p,f=\text{NEV}}(t) \cdot M_{\text{pack}} \cdot \eta_{\text{pack}}(t)}{EC_{p,f=\text{NEV}}(t) \cdot \alpha_{p,f=\text{NEV}}} \times 100\%$$
 (5 – 11)

The industry average cell energy density $ED_{avg}(t)$ is the market-share-weighted average of different technology pathways:

$$ED_{\text{avg}}(t) = \sum_{\varphi} s_{\varphi}(t) \cdot ED_{\varphi}(t)$$
 (5 – 12)

Here, $s_{\phi}(t)$ is the market share of technology ϕ (e.g., NMC, LFP, Li-S/Li-Air), and the specific energy density $ED_{\phi}(t)$ follows an S-curve of technological progress.

5.3.4. Refueling/Recharging convenience

Refueling/recharging convenience quantifies infrastructure accessibility and is crucial for NEV adoption. The convenience index for each province is defined by the ratio of infrastructure density to vehicle stock:

$$ERAI_{p,f}(t) = \frac{RI_{p,f}(t)/Area_p}{V_{p,f}(t)}$$
 (5 - 13)

Where $RI_{p,f}(t)$ is the number of refueling/recharging facilities (e.g., charging points, gas stations), Area_p the provincial area, and $V_{p,f}(t)$ is the vehicle ownership. Convenience for BEV is measured by the ratio of public charging point density to BEV stock; convenience for ICEV is measured by the ratio of gas station density to total ICEV ownership; convenience for PHEV considers the ratio combining private charging point density (relative to PHEV stock) and gas station density. The evolution of the vehicle-to-infrastructure ratio follows national planning targets. The ratio between public and private charging points, $\psi_p(t)$, is defined by system consistency constraints:

$$\frac{1}{R_{\text{public}}} = \frac{V_{p,f=\text{BEV}}(t) + V_{p,f=\text{PHEV}}(t)}{Charge_{\text{public}_p}(t)}$$
(5 - 14)

$$\frac{1}{R_{\text{private}}} = \frac{V_{p,f=\text{BEV}}(t) + V_{p,f=\text{PHEV}}(t)}{Charge_{\text{private}_p}(t)}$$
(5 - 15)

$$\frac{1}{R_{\text{total}}} = \frac{V_{p,f=\text{BEV}}(t) + V_{p,f=\text{PHEV}}(t)}{Charge_{\text{public}_p}(t) + Charge_{\text{private}_p}(t)}$$
(5 - 16)

$$\frac{1}{R_{\text{total}}} = \frac{1}{R_{\text{public}}} + \frac{1}{R_{\text{private}}}$$
 (5 – 17)

$$\Psi_p(t) = \frac{R_{\text{public}_p}(t)}{R_{\text{private}_n}(t)}$$
 (5 – 18)

5.4. Projection for buses and taxis

The projection for the public bus and taxi stock uses a demand-driven capacity planning model, implemented in three steps.

Predicting Public Transport Passenger Volume: Provincial public transport passenger volume is projected using multiple linear regression based on population, GDP per capita, and private car ownership. Regarding historical data, statistics before 2017 included buses/taxis and rail transit; post-2018 data are reported separately; from 2020, taxi and ferry passenger volumes are included. These changes are considered in our estimation.

Estimating Bus/Taxi Share: The variable 'share of bus/taxi passenger volume' is constructed. Its future trend is estimated using machine learning methods based on its historical nonlinear relationship with urbanization rates. This share is assumed to change dynamically with urbanization, considering factors like new subway line openings (e.g., assumed for Qinghai, Tibet around 2030).

Deriving Vehicle Stock from Service Intensity: The vehicle stock is derived using provincial 'service intensity' (passengers carried per vehicle per year). Service intensity is obtained by fitting the relationship between annual passenger volume and the number of operational vehicles over the past five years, using a weighted average

method. The future vehicle stock is then calculated based on the projected passenger volume and this service intensity.

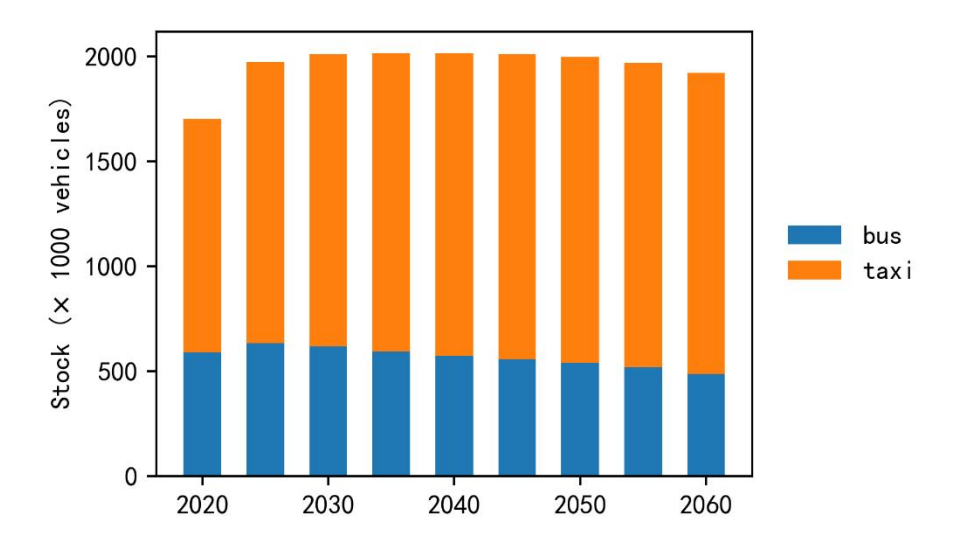


Figure 5-4 National bus and taxi stock forecast (2020-2060).

Table 5-3 Regional grouping based on subway availability.

Group	Description	Region	
G1	Subway opened early (<1997)	Beijing, Shanghai	
G2	Subway not yet opened (as of 2023)	Hainan, Qinghai, Tibet, Ningxia	
G3	Subway opened between 1997-2005	Guangdong, Tianjin, Hubei, Jilin, Liaoning, Jiangsu, Chongqing	
G4	Subway opened between 2009-2014	Sichuan, Henan, Heilongjiang, Zhejiang, Hunan, Shaanxi, Yunnan	
G5	Subway opened in 2015	Fujian, Jiangxi, Shandong	
G6	Subway opened between 2016-2021	Inner Mongolia, Anhui, Hebei, Guangxi, Gansu, Guizhou, Xinjiang, Shanxi	

References

AGICO Cement Plant Equipment (2025) *Lime Rotary Kiln*. Available at: https://cementplantequipment.com/products/lime-rotary-kiln/.

Arasto, A. (2015) "Techno-economic evaluation of significant CO2 emission reductions in the iron and steelindustry with CCS." Available at: https://publications.vtt.fi/pdf/science/2015/S111.pdf.

Bai C. and Zhang Q. (2017) "China's Growth Potential to 2050: A Supply-side Forecast Based on Cross-country Productivity Convergence and Its Featured Labor Force," *China Journal of Economics*, 4(4), pp. 1–27. Available at: https://doi.org/10.16513/j.cnki.cje.2017.04.001.

Baltac, S. et al. (2022) Low-Carbon Hydrogen from Natural Gas: Global Roadmap. 2022–07. Cheltenham, UK: IEA Greenhouse Gas R&D Programme (IEAGHG).

Available at: https://publications.ieaghg.org/technicalreports/2022-07%20Low-Carbon%20Hydrog en%20from%20Natural%20Gas%20Global%20Roadmap.pdf.

Benavides, K. *et al.* (2024) "Mitigating emissions in the global steel industry: Representing CCS and hydrogen technologies in integrated assessment modeling," *International Journal of Greenhouse Gas Control*, 131, p. 103963. Available at: https://doi.org/10.1016/j.ijggc.2023.103963.

Biomass Energy Industry Promotion Association *et al.* (2021) 3060 Blue Book of Zero-carbon Biomass Potential.

Biomass Energy Industry Promotion Association and Energy Foundation (2023) Strategic Positioning and Application Scenarios for Promoting Pollution Reduction and Carbon Emission Reduction through Clean Utilization of Biomass Energy.

Butterworth, P. (2024) *Challenges in achieving >90% carbon capture: Technical vs economic factors*. Available at: https://www.crugroup.com/cn/communities/thought-leadership/2024/Challenges-in-ac hieving-90percent-carbon-capture-Technical-vs-economic-factors/.

CEIC (2024) CEIC Open Data.

CEIC Data (2025) 中国—36 城工业用天然气平均价格(月度). Available at: https://www.ceicdata.com/zh-hans/china/price-monitoring-center-ndrc-36-city-monthl y-avg-transaction-price-production-material/cn-usage-price-36-city-avg-natural-gas-n atural-gas-for-industry.

Chen, Y. *et al.* (2020) "Provincial and gridded population projection for China under shared socioeconomic pathways from 2010 to 2100," *Scientific Data*, 7(1), p. 83. Available at: https://doi.org/10.1038/s41597-020-0421-y.

China Meteorological Administration (2023) *China Wind and Solar Energy Resources Bulletin (2022)*. Available at: https://www.cma.gov.cn/zfxxgk/gknr/qxbg/202304/t20230421_5454513.html (Accessed: October 15, 2024).

China Meteorological Administration (2025) *China Wind and Solar Energy Resources*Bulletin. Available at: https://www.cma.gov.cn/zfxxgk/gknr/qxbg/202502/t20250211_6847016.html (Accessed: October 17, 2025).

China National Administration of Coal Geology (2016) *China Occurrence Regularity of Coal Resources and Resource Evaluation*. Di 1 ban. Beijing: Science Press.

Chinese Academy of Environmental Planning (2024) *Assessment of Wind and Solar Power Generation Potential in China 2024*. Available at: https://www.caep.org.cn/sy/tdftzhyjzx/zxdt/202406/t20240614 1075803.shtml.

Christensen, P., Gillingham, K. and Nordhaus, W. (2018) "Uncertainty in forecasts of long-run economic growth," *Proceedings of the National Academy of Sciences*, 115(21), pp. 5409–5414. Available at: https://doi.org/10.1073/pnas.1713628115.

Christoph Heinemann et al. (2024) PTX Business Opportunity Analyser (BOA): Data Documentation. Documentation of data sources and data processing, version 2.1. Freiburg and Berlin, Germany: Oeko-Institut. Available at: https://www.agora-industry.org/fileadmin/Projects/2022/2022-01_INT_PtX-Dialog/O eko-Institut 2024 PTXBOA Data Documentation v 2.1.pdf.

Chumin (2025) *Maerz Vertical Calcination Lime Kiln Double Chamber Shaft HPS Operation*. TONGLI HEAVY MACHINERY. Available at: https://www.cementl.com/maerz-vertical-calcination-lime-kiln-double-chamber-shaft.

CSteelNews (2023) Daily Consumption of Sintered Fine Ore Increases and Domestic Pellet Proportion Increases--Analysis of Daily Consumption Structure of Iron Ore in Chinese Steel Enterprises in Late February 2023. Available at: http://www.csteelnews.com/xwzx/gdpl/202304/t20230406_73453.html.

CSteelNews (2025) *Domestic scrap market is weak*. Available at: http://www.csteelnews.com/sjzx/gsfx/202508/t20250827_103195.html.

Dianchacha (2024) *Power data platform*. Available at: https://www.dianchacha.cn (Accessed: October 21, 2024).

Ember (2023) *Global Electricity Review 2023*. EMBER. Available at: https://ember-energy.org/latest-insights/global-electricity-review-2023 (Accessed: November 29, 2024).

EMBER (2024) Global Electricity Review 2024. Ember.

Energy Transitions Commission (2023) *Making the Hydrogen Economy Possible: Accelerating Clean Hydrogen in an Electrified Economy* — *Technical Annex*. London, UK: Energy Transitions Commission. Available at: https://www.energy-transitions.org/wp-content/uploads/2023/04/2022-053-ETC-Hydrogen-Technical-Annex-Final .pdf.

European Commission. Joint Research Centre. (2022) *Greenhouse gas intensities of the EU steel industry and its trading partners*. LU: Publications Office. Available at: https://data.europa.eu/doi/10.2760/170198 (Accessed: August 29, 2025).

Gallaher, M.P., Depro, B.M. and Agency, U.S.E.P. (2002) *Economic Impact Analysis of the Final Coke Ovens NESHAP: Final Report*. EPA-452/R-02-008. Research Triangle Park, NC: U.S. Environmental Protection Agency, Office of Air Quality Planning and Standards. Available at: https://www.epa.gov/sites/default/files/2020-07/documents/coke-ovens_eia_neshap_final 08-2002.pdf.

Hanssen, S.V. *et al.* (2020) "The climate change mitigation potential of bioenergy with carbon capture and storage," *Nature Climate Change*, 10(11), pp. 1023–1029. Available at: https://doi.org/10.1038/s41558-020-0885-y.

He, Y. *et al.* (2025) "Decarbonization pathways and layout evolution in China's steel sector," *Renewable and Sustainable Energy Reviews*, 215, p. 115588. Available at: https://doi.org/10.1016/j.rser.2025.115588.

Huppmann, D. *et al.* (2019) "The MESSAGEix Integrated Assessment Model and the ix modeling platform (ixmp): An open framework for integrated and cross-cutting analysis of energy, climate, the environment, and sustainable development," *Environmental Modelling & Software*, 112, pp. 143–156. Available at: https://doi.org/10.1016/j.envsoft.2018.11.012.

IEA (2013) *Iron and Steel CCS Study (Techno-Economics Integrated Steel Mill.* Cheltenham, UK: IEA Greenhouse Gas R&D Programme. Available at: https://ieaghg.org/publications/iron-and-steel-ccs-study-techno-economics-integrated-steel-mill/.

IEA (2019) "The Future of Hydrogen." Available at: https://iea.blob.core.windows.net/assets/9e3a3493-b9a6-4b7d-b499-7ca48e357561/Th e Future of Hydrogen.pdf.

IEA (2020) Global average levelised cost of hydrogen production by energy source and technology, 2019 and 2050 – Charts – Data & Statistics, IEA. Available at: https://www.iea.org/data-and-statistics/charts/global-average-levelised-cost-of-hydrog en-production-by-energy-source-and-technology-2019-and-2050 (Accessed: October 18, 2025).

IEA (2022) World Energy Outlook 2022.

IEA (2023a) *Energy Technology Perspectives 2023*. Available at: https://www.iea.org/reports/energy-technology-perspectives-2023 (Accessed: December 3, 2024).

IEA (2023b) World Energy Investment 2024. IEA.

IEA (2024) ETP Clean Energy Technology Guide – Data Tools, IEA. Available at: https://www.iea.org/data-and-statistics/data-tools/etp-clean-energy-technology-guide (Accessed: November 30, 2024).

IEA Greenhouse Gas R&D Programme (2024) Clean Steel: an Environmental and Technoeconomic Outlook of a Disruptive Technology. 2024–02. IEA GBHG R&D Programme. Available at: https://publications.ieaghg.org/technicalreports/2024-02%20Clean%20Steel%20An% 20environmental%20and%20technoeconomic%20outlook%20of%20a%20disruptive %20technology.pdf.

IEA-ETSAP (2010a) *Iron and Steel: Highlights*. IEA-ETSAP (Energy Technology Systems Analysis Programme). Available at: https://iea-etsap.org/E-TechDS/HIGHLIGHTS%20PDF/I02-Iron%26Steel-GS-AD-gc t%201.pdf.

IEA-ETSAP (2010b) *Iron and Steel: Highlights*. IEA-ETSAP (Energy Technology Systems Analysis Programme). Available at: https://iea-etsap.org/E-TechDS/HIGHLIGHTS%20PDF/I02-Iron%26Steel-GS-AD-gc t%201.pdf.

IIASA ECE Programme (2020) Documentation of the MESSAGEix framework.

Jing, C. *et al.* (2022) "Gridded value-added of primary, secondary and tertiary industries in China under Shard Socioeconomic Pathways," *Scientific Data*, 9(1), p. 309. Available at: https://doi.org/10.1038/s41597-022-01440-0.

Kang, Y. *et al.* (2020) "Bioenergy in China: Evaluation of domestic biomass resources and the associated greenhouse gas mitigation potentials," *Renewable and Sustainable Energy Reviews*, 127, p. 109842. Available at: https://doi.org/10.1016/j.rser.2020.109842.

kq81.com (2025) *Limestone Price Quotes for Aug 19*. Available at: https://www.kq81.com/AspCode/KyxtShow.asp?ArticleId=534897.

Leimbach, M. *et al.* (2017) "Future growth patterns of world regions – A GDP scenario approach," *Global Environmental Change*, 42, pp. 215–225. Available at: https://doi.org/10.1016/j.gloenvcha.2015.02.005.

Li, J. (2019) Fourth Assessment for Oil and Gas Resource. Beijing: Petroleum Industry Press.

Lu, X. *et al.* (2021) "Combined solar power and storage as cost-competitive and grid-compatible supply for China's future carbon-neutral electricity system," *Proceedings of the National Academy of Sciences*, 118(42), p. e2103471118. Available at: https://doi.org/10.1073/pnas.2103471118.

McElroy, M.B. *et al.* (2009) "Potential for Wind-Generated Electricity in China," *Science*, 325(5946), pp. 1378–1380. Available at: https://doi.org/10.1126/science.1175706.

McGlade, C. and Ekins, P. (2015) "The geographical distribution of fossil fuels unused when limiting global warming to 2 °C," *Nature*, 517(7533), pp. 187–190. Available at: https://doi.org/10.1038/nature14016.

Ministry of Natural Resources of the People's Republic of China (2021) *National Petroleum and Natural Gas Resources Exploration and Mining Reports* 2020. Available at: http://gi.m.mnr.gov.cn/202109/t20210918_2681270.html (Accessed: August 5, 2024).

Nancy Margolis and Ross Brindle (2000) *Energy and Environmental Profile of the U.S. Iron and Steel Industry*. Energetics, Incorporated. Available at: https://www.energy.gov/sites/prod/files/2013/11/f4/steel_profile.pdf.

National Bureau of Statistics of China (2022) *China Statistical Yearbook 2022*. Available at: https://www.stats.gov.cn/sj/ndsj/2022/indexch.htm (Accessed: December 3, 2024).

National Bureau of Statistics of China (2023) *China Statistical Yearbook 2023*. Available at: https://www.stats.gov.cn/sj/ndsj/2023/indexch.htm (Accessed: December 3, 2024).

National Bureau of Statistics of China (2024) *China Statistical Yearbook 2024*. Available at: https://www.stats.gov.cn/sj/ndsj/2024/indexch.htm (Accessed: December 3, 2024).

National Bureau of Statistics of China (2025) *Market price changes of important means of production in circulation in mid-January 2025*. Available at: https://www.stats.gov.cn/sj/zxfb/202501/t20250123 1958423.html.

- Nie, Y. *et al.* (2020) "Spatial distribution of usable biomass feedstock and technical bioenergy potential in China," *GCB Bioenergy*, 12(1), pp. 54–70. Available at: https://doi.org/10.1111/gcbb.12651.
- OECD (2025) *Hydrogen in steel: Addressing emissions and dealing with overcapacity.* 174th ed. OECD Science, Technology and Industry Policy Papers. Available at: https://doi.org/10.1787/7e2edc69-en.
- O'Neill, B.C. *et al.* (2014) "A new scenario framework for climate change research: the concept of shared socioeconomic pathways," *Climatic Change*, 122(3), pp. 387–400. Available at: https://doi.org/10.1007/s10584-013-0905-2.
- O'Neill, B.C. *et al.* (2017) "The roads ahead: Narratives for shared socioeconomic pathways describing world futures in the 21st century," *Global Environmental Change*, 42, pp. 169–180. Available at: https://doi.org/10.1016/j.gloenvcha.2015.01.004.
- Pan J. et al. (2020) "Spatio-temporal changes of output value from the primary, secondary and tertiary industries for 2020-2050 under the Shared Socioeconomic Pathways," Climate Change Research, 16(6), pp. 725–737.

Rahbari, A. *et al.* (2025) "Solar-thermal sintering of iron ore," *Solar Energy*, 286, p. 113123. Available at: https://doi.org/10.1016/j.solener.2024.113123.

Rechberger, K. *et al.* (2020) "Green Hydrogen-Based Direct Reduction for Low-Carbon Steelmaking," *steel research international*, 91(11), p. 2000110. Available at: https://doi.org/10.1002/srin.202000110.

Reliable Plant (2008) *Sunoco to build coke facility in Granite City, Illinois*. Available at: https://www.reliableplant.com/Read/11674/sunoco-to-build-coke-facility-in-granite-city%2C-illinois.

Renmin University of China (2025) *CPOST documentation*. Available at: http://ae.ruc.edu.cn/docs/2025-02/55f9843587594f7ba4975a1124c964f9.pdf (Accessed: September 7, 2025).

Santos, S. et al. (2013) Understanding the Cost of Deploying CO2 Capture in an Integrated Steel Mill. IEA Greenhouse Gas R&D Programme. Available at: https://publications.ieaghg.org/docs/General_Docs/IEAGHG_Presentations/S._Santos ESTEP Mtg IS ppt final.pdf.

Shao Le *et al.* (2024) "Economic analysis of hydrogen production from coal, natural gas and green electricity," *Refining and Chemical Industry*, 35(2), pp. 10–14. Available at: https://doi.org/10.16049/j.cnki.lyyhg.2024.02.013.

Shenlan Environmental Protection Industry Development Co., Ltd. (2025) *Cement industry, why become global carbon emissions "hot potato"?* Available at: https://mp.weixin.qq.com/s/Tq6LJxZq ATvOirTzWteeA.

State-owned Assets Supervision and Administration Commission of the State Council (2020) "Circular on Printing and Distributing the Operational Guidelines for the Reform of Mixed Ownership of Central Enterprises." Available at: https://www.gov.cn/guowuyuan/2019-11/10/content 5450524.htm.

Steelonthenet (2023) Examples of capital investment costs for iron and steelmaking.

Available at: https://www.steelonthenet.com/pdf/commerce/capex examples.pdf.

Steelonthenet (2025) *Steel Industry Scope 1 CO2 Emissions by Process Step.* Available at: https://www.steelonthenet.com/kb/scope-1-emissions.html.

steelonthenet (no date) *Steel Industry Scope 1 CO2 Emissions by Process Step.* Available at: https://www.steelonthenet.com/kb/scope-1-emissions.html.

Steelonthenet.com (2025) "Iron & steel industry capital investment cost database." Available at: https://www.steelonthenet.com/capital-investment/eaf.html.

Tian, Y. et al. (2021) "Development Strategy of Biomass Economy in China," Strategic Study of CAE, 23(1), pp. 133–140.

Trading Economics (2025) *Iron Ore - 价格数据与图表*. Available at: https://zh.tradingeconomics.com/commodity/iron-ore.

UN DESA/Population Division (2024) World Population Prospects 2024: Summary of Results.

Vogl, V., Åhman, M. and Nilsson, L.J. (2018) "Assessment of hydrogen direct reduction for fossil-free steelmaking," *Journal of Cleaner Production*, 203, pp. 736–745. Available at: https://doi.org/10.1016/j.jclepro.2018.08.279.

Wang Rui et al. (2023) "A high spatial resolution dataset of China's biomass resource potential," Scientific Data, 10(1). Available at:

 $https://kns.cnki.net/kcms2/article/abstract?v=S8jPpdFxNHiTQVeImBYK8mA-BDX9\\8bt1ba36wSf_58WTl8McZReeDpIPpFV2AKyPI9C7qpTScUVZj0x5Cv3s99ThPeWlDVq0aV_2fYsUpxh8eR-sCGLGE1UQy1yjKc1H9hF8PyXLulOJ47DPYW2gPw=&uniplatform=NZKPT&language=gb.$

- Wang, Y. et al. (2022) "Assessment of wind and photovoltaic power potential in China," Carbon Neutrality, 1(1), p. 15. Available at: https://doi.org/10.1007/s43979-022-00020-w.
- Wang, Y. *et al.* (2025) "Long-term transformation in China's steel sector for carbon capture and storage technology deployment," *Nature Communications*, 16(1), p. 4251. Available at: https://doi.org/10.1038/s41467-025-59205-3.
- Welsby, D. *et al.* (2021) "Unextractable fossil fuels in a 1.5 °C world," *Nature*, 597(7875), pp. 230–234. Available at: https://doi.org/10.1038/s41586-021-03821-8.
- Yang Y. *et al.* (2024) "National and provincial economy projection databases under Shared Socioeconomic Pathways (SSP1-5)_v2," *Climate Change Research*, 20(4), pp. 498–503.
- Zhang, B. (2018) Assessment of Raw Material Supply Capability and Energy Potential of Biomass Resources in China. PhD thesis. China Agricultural University. Available at: https://kns.cnki.net/kcms2/article/abstract?v=FC2wxXHna7pdQvqTGMfmETRMzybZx6gtubt6mbrheQJIq-ZBFX2DvoVEsT-o4n9Z2bom8YJuzaK2PHHojDPL7zt80vmC0ZnQXQVIwevLYzZi21w37f6bxOurUyLp0hfV&uniplatform=NZKPT&language=gb.
- Zhang, Q.-Z. *et al.* (2024) "Analysis of hydrogen supply and demand in China's energy transition towards carbon neutrality," *Advances in Climate Change Research*, 15(5), pp. 924–935. Available at: https://doi.org/10.1016/j.accre.2024.07.013.
- ZHAO Zedong, LI Jiaxuan, and LI Yuanye (2025) "Practice of Low-Carbon Production in Modern Long-Process Steel Enterprises," *Metallurgical Power*, (4), pp. 83–87. Available at: https://doi.org/10.13589/j.cnki.yjdl.2025.04.002.